



ISSN: 0067-2904
GIF: 0.851

Peristaltic Transport for Fractional Generalized Maxwell Viscoelastic Fluids through a Porous Medium in an Inclined Channel with Slip Effect

Lika Z. Hummady^{1*}, Ahmed M. Abdulhadi²

¹Department of Geology, College of Science, University of Baghdad, Baghdad, Iraq

²Department of Mathematics, College of Science, University of Baghdad, Baghdad, Iraq

Abstract

In this paper we present a study on Peristaltic of fractional generalized Maxwell viscoelastic fluid through a porous medium. A modified Darcy-Brinkman model is utilized to simulate the flow of a generalized Maxwell fluid in a porous medium in an inclined channel with slip effect. The governing equation is simplified by assuming long wavelength and low Reynolds number approximations. The numerical and approximate analytical solutions of the problem are obtained by a semi-numerical technique, namely the homotopy perturbation method. The influence of the dominating physical parameters such as fractional Maxwell parameter, relaxation time, amplitude ratio, permeability parameter, Froude number, Reynolds number and inclination of channel on the flow characteristics are depicted graphically.

Keywords: Peristaltic Transport, fractional generalized Maxwell, Slip effect, Porous Medium, Inclined a symmetric channel, pinging, trapping.

النقل المتمعج لمعجم ماكسويل الكسري للسوائل اللزجة من خلال وسط مسامي في قناة مائلة مع تأثير الانزلاق

لقاء زكي حمادي^{1*} ، احمد مولود عبد الهادي²

¹قسم علوم الارض، كلية العلوم، جامعه بغداد، بغداد، العراق

²قسم الرياضيات، كلية العلوم، جامعه بغداد، بغداد، العراق

الخلاصة

في هذه البحث تم تقديم دراسة عن الحركة التموجية الانتقاليه للسوائل اللزجة من معجم ماكسويل من خلال وسيط يسهل اختراقها . ويستخدم لتعديل نموذج دارسي برينكمان لمحاكاة تدفق سائل ماكسويل المعجم في وسط مسامي في قناة مائلة مع تأثير الانزلاق . الدراسة تمت تحت فرضيه طول موجي طويل وفرضيه ان يكون عدد رينولدز صغير. ويتم الحصول على الحلول التحليلية و العددية التقريبية لهذه المساله من خلال تقنية شبه العددية ، وهي طريقة اضطراب هوموتوبي . تأثير الاعداد اللابيديه ; كسور المشتقات الجزئية لماكسويل المعجم ، وقت الاسترخاء ، نسبة السعة ، المعلمة النفاذية، فرويد العدد، رقم رينولدز و زاويه ميل القناة ، السعه على اختلاف الضغط ، قوه الاحتكاك وداله الجريان قد تم ايجادها وتحليلها .

1. Introduction

Non-Newtonian characteristics are exhibited by numerous fluids including physiological liquids (blood, food bolus, chime), geological suspensions (drilling muds, sedimentary liquids), industrial tribological liquids (oil and greases), and biotechnological liquids (biodegradable polymers, gels, food stuffs). It is difficult to propose a single model which can exhibit all the properties of non-Newtonian fluids. To describe the viscoelastic properties of such fluids recently, constitutive equations with ordinary and fractional time derivatives have been introduced. Fractional calculus has proved to be

*Email: geomythlika@scbaghdad.edu.iq

very successful in the description of constitutive relations of viscoelastic fluids. The starting point of the fractional derivative model of viscoelastic fluids is usually a classical differential equation which is modified by replacing the time derivative of an integral order with fractional order and may be formulated both in the Riemann-Liouville or Caputo sense [1].

This generalization allows one of define precisely non-integer order integrals or derivatives. Considering the relevance of fractional models of viscoelastic fluids, a number of articles [2-8], have addressed unsteady flows of viscoelastic fluids in conduits with the fractional Maxwell model, fractional generalized Maxwell model, fractional second grade fluid, fractional Oldroyd-B model, fractional Burgers model, or generalized Burgers' fractional model for a variety of different geometries for wall surface. Solutions for the velocity field and the associated shear stress in such studies have frequently been obtained by using various transforms including the Laplace transform, Fourier transform, Weber transform, Hankel transform or discrete Laplace transform methods. Oscillating (or transient) flow of non-Newtonian fluids through a channel or tube is a fundamental flow regime encountered in many biological and industrial transport processes.

The quasi-periodic blood flow in the cardiovascular system, movement of food bolus in the gastrointestinal tract and urodynamics transport in the human ureter are just several example of oscillating flow in biological systems. Industrial application of oscillating flows includes slurry and waste conveyance systems employing roller pumping and finger pumps. The low Reynolds numbers characterizing such flows, and the fact that, the dimensions of the channel and macromolecules in the fluid can be of the same order of magnitude, can lead to effects unseen in macroscopic systems.

As the fractional models have been studied extensively in recent years in biomedical transport problems [9], [10] investigated the peristaltic flow of fractional Maxwell fluid through a channel. Further studies have utilized the generalized fractional Maxwell model, fractional Oldroyd-B model, and fractional Burgers' model [11] in a variety peristaltic flow configurations.

Some semi-numerical and analytical methods including the homotopy perturbation method (HPM), homotopy analysis method (HAM), variational iteration method (VIM), and adomian decomposition method (ADM) have been employed to obtain robust solution of fractional partial differential equation (FPDE). Perturbation method is one of the well-known methods to solve these kinds of nonlinear equations and was studied by number of research [12, 13]. Since there are some limitations with the common perturbation method also, because the basis of the common perturbation method was upon the existence of a small parameter, developing the methods for different applications is very difficult. Therefore, many different new methods have been introducing recently and some new ways to eliminate the small parameter have been introduced, including artificial parameter method by [14], the variation iteration method by [15,16] and the homotopy-perturbation method by [17].

To the best knowledge of the authors, no studies thus far examined analytically the oscillating flow of generalized Maxwell fluids through a porous medium in an inclined channel. In this paper studied this case and furthermore employ the HPM to derive approximate analytical solution. Numerical results for different cases are depicted graphically.

2. Definitions

2.1 Gamma function

The gamma function $\Gamma(z)$ is defined by the integral

$$\Gamma(z) = \int_0^{\infty} \exp(-t)t^{z-1} dt. \quad (1)$$

Some of common properties of gamma function are

i- $\Gamma(n+1) = n\Gamma(n)$

ii- $\Gamma(n+1) = n!$

2.2 Riemann-Liouville fractional integral

Let $R(v) > 0$ and let f be piecewise continuous on $(0, \infty)$ and integrable on any finite subinterval of $[0, \infty)$. Then for $t > 0$ we call

$${}_0 D_t^{-v} f(t) = \frac{1}{\Gamma(v)} \int_0^t (t-\xi)^{v-1} f(\xi) d\xi \quad (2)$$

The Riemann-Liouville fractional integral of f of order v .

2.3 Fractional derivative

Let f be a function of class C and let $\omega > 0$. Let m be the smallest integer that exceeds ω . Then the fractional derivative of f of order ω is defined as:

$$D^\omega f(t) = D^m [D^{-\nu} f(t)], \quad \omega > 0, \quad t > 0, \tag{3}$$

(If exists) where $\nu = m - \omega > 0$.

3. Mathematical Model

The constitutive equation for shear stress-strain relationship of viscoelastic fluids obeying the fractional Maxwell model [1], [18] are given by:

$$(1 + \lambda_1^{-\gamma} \frac{\partial^\gamma}{\partial t^\gamma}) \bar{\tau} = \mu \dot{\gamma} \tag{4}$$

Where $\bar{\lambda}_1, \bar{t}, \bar{\tau}, \mu, \dot{\gamma}$ are the relaxation time, shear stress, viscosity and the rate of shear strain respectively, and γ is fractional parameter such that $0 \leq \gamma \leq 1$. If $\gamma = 0$, this model reduces to the classical Newtonian model and when $\gamma = 1$, the model reduces to the Maxwell model.

The fractional parameter γ characterizes the rheological behavior of materials that is intermediate between the Newtonian and Maxwell viscoelastic fluids. This model is composed of a Hooke element connected in series with a Scott-Blair element. The details are given in [1].

The well-known Darcy law states that, for the flow of a Newtonian fluid through a porous medium, the pressure gradient caused by the fractional drag is directly proportional to the velocity. Recently, based on the local volume averaging technique and balance of the forces acting on volume element of viscoelastic fluids in porous media, [19] developed a modified Darcy-Brinkman model for flows of some models of viscoelastic fluids in porous media. Darcy resistance quantifies the impedance to the flow in the bulk of the porous space. For generalized Maxwell fluid flows in porous media, the Darcy resistance [18] can be expressed as follows:

$$(1 + \lambda_1^{-\gamma} \frac{\partial^\gamma}{\partial t^\gamma}) R = \frac{\mu \phi}{k} \bar{u} \tag{5}$$

Where R, ϕ, k and \bar{u} designate the Darcy resistance, porosity of the porous medium, permeability, and axial velocity, respectively. Figure-1 shows the geometry of oscillating flow through a porous medium, for the present problem.

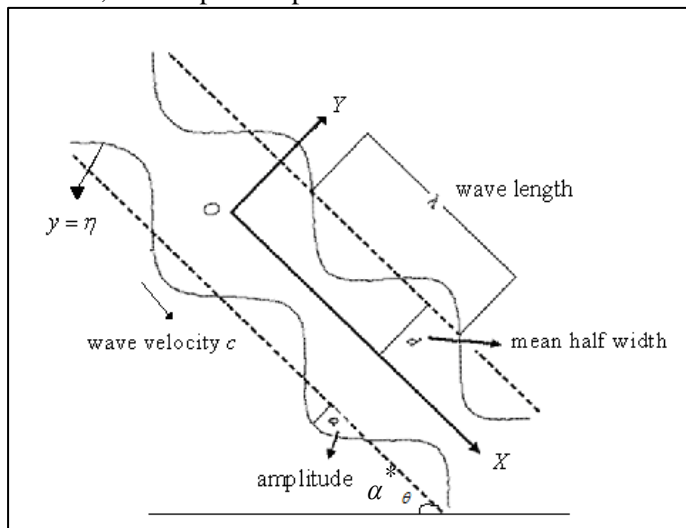


Figure 1- Geometry of the two dimensional peristaltic transport in an inclined channel

The constitutive equation for the geometry under consideration Figure-1, i.e., oscillating peristaltic flow through a uniform porous medium takes the form:

$$\bar{h}(x, t) = a - \frac{1}{2} \phi (1 + \cos \frac{2\pi}{\lambda} (x - ct)) \tag{6}$$

Where $\bar{h}, \lambda, a, c, \bar{\phi}$ are the transverse oscillating displacement, wavelength, half-width of the channel, wave velocity and amplitude, respectively. This model reduce to ordinary Newtonian model if $\gamma = 0$ and classical Navier Stokes motion in horizontal channel when $\alpha^* = 0$.

4. Governing equation

The governing equations of motion in an inclined channel for generalized Maxwell fluid flow through a porous medium using the above formulations can be shown to take the form:

$$\frac{\partial \bar{u}}{\partial x} + \frac{\partial \bar{v}}{\partial y} = 0 \tag{7}$$

$$\rho \left(\frac{\partial}{\partial t} + u \frac{\partial}{\partial x} + v \frac{\partial}{\partial y} \right) \bar{u} = - \frac{\partial \bar{p}}{\partial x} + \frac{\partial \bar{\tau}_{xx}}{\partial x} + \frac{\partial \bar{\tau}_{xy}}{\partial y} + R_x + \rho g \sin \alpha^* \tag{8}$$

$$\rho \left(\frac{\partial}{\partial t} + u \frac{\partial}{\partial x} + v \frac{\partial}{\partial y} \right) \bar{v} = - \frac{\partial \bar{p}}{\partial y} + \frac{\partial \bar{\tau}_{xy}}{\partial x} + \frac{\partial \bar{\tau}_{yy}}{\partial y} + R_y - \rho g \cos \alpha^* \tag{9}$$

Introducing the following dimensionless parameters:

$$h = \frac{\bar{h}}{a}, t = \frac{c\bar{t}}{\lambda}, p = \frac{\bar{p}a^2}{\mu c \lambda}, \delta = \frac{a}{\lambda}, k = \frac{\phi k}{a^2}, \lambda_1 = \frac{c\lambda_1}{\lambda}, Fr = \frac{c^2}{ga} \tag{10}$$

$$\tau = \frac{a\bar{\tau}}{\mu c}, x = \frac{\bar{x}}{\lambda}, y = \frac{\bar{y}}{a}, u = \frac{\bar{u}}{c}, v = \frac{\bar{v}}{c\delta}, \phi = \frac{\bar{\phi}}{a}, Re = \frac{\rho ca}{\mu}$$

where $h, \delta, k, \lambda_1, Fr, \tau, \phi, Re$, are the ratio of the width of channels, the wave number, permeability parameter, wave number, Froude number, shear stress, amplitude ratio, Reynolds number respectively.

Substitute the values of shear stress and Darcy resistance from Eqs.(4) and (5) into Eqs.(7), (8),(9) using the non-dimensional parameters from Eq.(10) we get:

$$(1 + \lambda_1^\gamma \frac{\partial^\gamma}{\partial t^\gamma}) \left(\frac{\partial p}{\partial x} - \frac{Re}{Fr} \sin \alpha^* \right) = \frac{\partial^2 u}{\partial y^2} - \frac{u}{k} \tag{11}$$

$$\frac{\partial p}{\partial y} = 0 \tag{12}$$

The associated boundary conditions are

$$\left. \frac{\partial u(x, y, t)}{\partial y} \right|_{y=0} = 0$$

$$u(x, y, t) \Big|_{y=h} = -\beta \frac{\partial u}{\partial y} \tag{13}$$

$$\left. \frac{\partial p}{\partial x} \right|_{y=0} = 0$$

Integrating Eqs.(11) ,(12) with respect to y and using the first and second condition of Eq.(13), the axial velocity is obtained as follows:

$$u = \left(\frac{-(1 + \lambda_1^\gamma \frac{\partial^\gamma}{\partial t^\gamma}) (\frac{\partial p}{\partial x} - \frac{Re}{Fr} \sin \alpha^*)}{w^2} \right) (1 + f(x)) \frac{\cosh wy}{\cosh wh} \tag{14}$$

$$f(x) = 1 + \beta f_1(x)$$

$$f_1(x) = \frac{\tan wh}{w}$$

The volume flow rate is defined as $Q = \int_0^h u dy$, which by virtue of Eq.(11), reduces to

$$Q = \frac{(1 + \lambda_1^\gamma \frac{\partial^\gamma}{\partial t^\gamma}) (\frac{\partial p}{\partial x} - \frac{Re}{Fr} \sin \alpha^*)}{w^2} (h + f(x) f_1(x)) \tag{15}$$

The transformations between the wave and the laboratory frames, in the dimensionless form, are given by $X = x - t, Y = y, U = u - 1$. (16)

Using the transformations defined in Eq.(16) it follows that Eq.(6) can be reduced to

$$h(x, t) = 1 - \phi \cos^2 \pi(x - t) \tag{17}$$

The volumetric flow rate in the wave frame is given by

$$q = \int_0^h U dY = \int_0^h (u - 1) dy \tag{18}$$

Which, on integration, yields

$$q = Q - h \tag{19}$$

The averaged flow rate Q_1 is defined as $Q_1 = \int_0^1 Q dt$ from (16) we have $Q = q + h$ hence

$$Q_1 = \int_0^1 (q + h) dt = q + 1 - \frac{\phi}{2} \tag{20}$$

Then, we get

$$Q = Q_1 - 1 + \frac{\phi}{2} + h \tag{21}$$

$$(1 + \lambda_1^\gamma \frac{\partial^\gamma}{\partial t^\gamma}) (\frac{\partial p}{\partial x} - \frac{Re}{Fr} \sin \alpha^*) = \frac{w^2 (Q_1 - 1 + \frac{\phi}{2} + h)}{(h + f(x) f_1(x))} \tag{22}$$

Using Eqs. (14) and (22), the stream function (ψ) in the wave frame given by ($U = \frac{\partial \psi}{\partial y}$) is obtained as

$$\psi = \frac{(Q_1 + h - 1 + \frac{\phi}{2})}{h + f(x) f_1(x)} [y + f(x) (\frac{\sinh(wy)}{\cosh(wh)})] - y \tag{23}$$

It is evident from Eq.(23) that the stream function is independent of fractional parameter and relaxation time and inclined channel.

5. (HPM) Solutions

To solve the governing equation the method of Homotopy perturbation method (HPM) will be used. Equation(18) can be rewritten as

$$\frac{\partial^\gamma}{\partial t^\gamma} \left(\frac{\partial p}{\partial x} - \frac{\text{Re}}{Fr} \sin \alpha^* \right) + \frac{1}{\lambda_1^\gamma} \frac{\partial p}{\partial x} - \frac{\text{Re}}{Fr} \sin \alpha^* = \frac{w^2 (Q_1 - 1 + \frac{\phi}{2} + h)}{(h + f(x))f_1(x)} \tag{24}$$

Equation (23) can be simplified to yield

$$D_t^\gamma f + \frac{1}{\lambda_1^\gamma} f = -\frac{A}{\lambda_1^\gamma} \tag{25}$$

Where $f(x,t) = \frac{\partial p}{\partial y} - \frac{\text{Re}}{Fr} \sin \alpha^*$ and $A = \frac{w^3 (Q_1 - 1 + \frac{\phi}{2} + h)}{(\tan wh - wh)}$ with initial condition

$$f(x,0) = \frac{\text{Re}}{Fr} \sin \alpha^* \tag{26}$$

According to the HPT given by [36]. We construct the following homotopy:

$$D_t^\gamma f = -q \left[\frac{1}{\lambda_1^\gamma} f + \frac{A}{\lambda_1^\gamma} \right] \tag{27}$$

Furthermore [15], we use the homotopy parameter " q " to expand the solution:

$$f = f_0 + q f_1 + q^2 f_2 + q^3 f_3 + \dots \tag{28}$$

When $q \rightarrow 1$ Eq.(28) becomes the approximation of Eq.(25). Substituting Eq.(28) into Eq.(27)

and comparing the like powers of q , we obtain the following set of fractional partial differential equation(FPDE):

$$\begin{aligned} q^0 : D_t^\gamma f_0 &= 0 \\ q^1 : D_t^\gamma f_1 &= -\frac{1}{\lambda_1^\gamma} f_0 - \frac{A}{\lambda_1^\gamma} \\ q^2 : D_t^\gamma f_2 &= -\frac{1}{\lambda_1^\gamma} f_1 \\ q^3 : D_t^\gamma f_3 &= -\frac{1}{\lambda_1^\gamma} f_2 \\ q^4 : D_t^\gamma f_4 &= -\frac{1}{\lambda_1^\gamma} f_3 \end{aligned} \tag{29}$$

And so on the method is based on applying the operator J_t^γ (the inverse operator of the Caputo derivative $D_t^\gamma f$) on both sides of Eq.(29), which leads to:

$$\begin{aligned}
 f_0 &= \frac{\text{Re}}{Fr} \sin \alpha^* \\
 f_1 &= -\frac{A}{\lambda_1^\gamma} \frac{t^\gamma}{\Gamma(\gamma + 1)} \\
 f_2 &= \frac{A}{\lambda_1^{2\gamma}} \frac{t^{2\gamma}}{\Gamma(2\gamma + 1)} \\
 f_3 &= -\frac{A}{\lambda_1^{3\gamma}} \frac{t^{3\gamma}}{\Gamma(3\gamma + 1)} \\
 f_4 &= \frac{A}{\lambda_1^{4\gamma}} \frac{t^{4\gamma}}{\Gamma(4\gamma + 1)}
 \end{aligned}
 \tag{30}$$

Thus, the exact solution may be obtained as

$$f(x, t) = \sum_{r=0}^{\infty} f_r = \sum_{r=0}^{\infty} [\varepsilon(\gamma)]^r \frac{t^{r\gamma}}{\Gamma(r\gamma + 1)},
 \tag{31}$$

Where

$$[\varepsilon(\gamma)]^r = \begin{cases} (-1)^r \frac{A}{\lambda_1^{r\gamma}}, & r \geq 1 \\ 0, & r = 0 \end{cases} = E_\gamma(\varepsilon(\gamma)t^\gamma)
 \tag{32}$$

Where $E_\gamma(t) = \sum_{r=0}^{\infty} \frac{t^r}{\Gamma(r\gamma + 1)}$, ($\gamma > 0$) is the Mittag-Leffler function in one parameter.

The pressure difference across one wave length (Δp) and the fractional force across one wavelength (F) are defined by the following integrals:

$$\begin{aligned}
 \Delta p &= \int_0^1 \frac{\partial p}{\partial x} dx \\
 F &= \int_0^1 h \left(-\frac{\partial p}{\partial x} \right) dx
 \end{aligned}
 \tag{33}$$

(34)

6. Numerical results and discussion

Numerical results have been presented in this section to study the effect of fractional viscoelastic behavior on oscillating peristaltic flow through a porous medium in an inclined channel with slip effect. Mathematica software is used to plot all the figures and 100 terms of mittag-Leffler function have been employed in the computations. All figures have been plotted based on Eqs.(33) & (34). The graphical plots are presented for the effects of relevant value of control parameters, i.e., the relaxation time (λ_1), fractional parameter (γ), slip parameter (β), permeability parameter (k), amplitude ratio(ϕ),

Renold number (Re), Froud number (Fr) and inclined channel (α^*). The salient feature of peristaltic transport for fractional generalized Maxwell viscoelastic fluids through a porous medium in an inclined channel are discussed through Figures From (2-19).

6.1 The Pressure Rise Distribution:

Figures from (2-9) are drawn between pressure difference across one wavelength and averaged flow rate. The variations of the volumetric flow rate of peristaltic waves with pressure gradient for different values of parameters are studied through these figures. These figures demonstrate that here is a linear relation between pressure and average flow rate. In Figure-2 we can see that with increases the Renold number (Re), the volumetric flow rate gradually decreasing in the entire pumping region, free pumping region and in co-pumping. In Figure-3 shows that, with increases the fractional parameter (γ), the volumetric flow rate gradually increasing in the entire pumping with free pumping but the volumetric flow rate decreasing in co-pumping. Figure-4 we see that, when increasing the slip parameter (β), the volumetric flow rate can be gradually reduced in the entire pumping region and the free pumping region but increasing in co-pumping region. Figure-5 we see that, with increases the permeability parameter (k), the volumetric flow rate can be gradually reduced in the entire pumping region and the free pumping region but increasing in co-pumping region. Figure-6 shows that, with the rise in the relaxation time (λ_1), the volumetric flow rate decreases in the pumping region and in free pumping and co-pumping the flow rate increasing. Figure-7 shows that, when the Froud number (Fr) increases, the volumetric flow rate increasing in the pumping region, free pumping region and in co-pumping region. Figure-8 shows that, when the inclined channel parameter (α^*) increases, the volumetric flow rate decreasing in the pumping region, free pumping region and in co-pumping region. Figure-9 shows that, when the magnitude of amplitude ratio increases, the volumetric flow rate is increasing in the pumping region and free pumping region but in co-pumping region the volumetric flow rate decreasing.

6.2 The Frictional force distribution:

Frictional force (F) in the case of fractional Maxwell fluid with an inclined channel is calculated over one wave period in the term of averaged volume flow rate. Figures From (10-17) are illustrated to show the variation of frictional force with averaged flow rate for different values pertinent parameters. It can be seen that the effect of increasing the flow rate is to enhance the frictional force. In Figure-10 we can see that with increases the Renold number (Re), the fractional force gradually increasing. In Figure-11 shows that, with increases the fractional parameter (γ), the fractional force gradually decreasing at $Q1 < 0.25$ but the fractional force increasing $Q1 > 0.25$. Figure-12 we see that, with increases the slip parameter (β), the fractional force can be gradually rise at $Q1 < 0.25$ but decreasing at $Q1 > 0.25$. Figure-13 we see that, with increases the permeability parameter (k), the fractional force can be gradually rise at $Q1 < 0.25$ but decreasing at $Q1 > 0.25$. Figure-14 shows that, with the rise in the relaxation time (λ_1), the fractional fore increases at $Q1 < 0.25$ and at $Q1 > 0.25$ the fractional force decreasing. Figure-15 shows that, when the Froud number (Fr) increases, the fractional force decreasing. Figure-16 shows that, when the inclined channel parameter (α^*) increases, the fractional force increasing. Figure-17 shows that, when the magnitude of amplitude ratio increases, fractional force decreasing.

6.3 The streamline distribution

The streamline on the center line in the wave frame reference are found to split in order to enclose a bolus of fluid particles circulating along closed streamline under certain conditions. This phenomenon is referred to as trapping, which is a characteristic of peristaltic motion. Since this bolus appears to be trapped by the wave, the bolus moves with the same speed as that of the wave. Figure-18 and -19 drawn for streamline patterns. The impacts of permeability parameter and slip parameter on trapping are discussed through these figures. It is important to observe that the size of trapping bolus reduces when the magnitude of said parameters (k and β) increases.

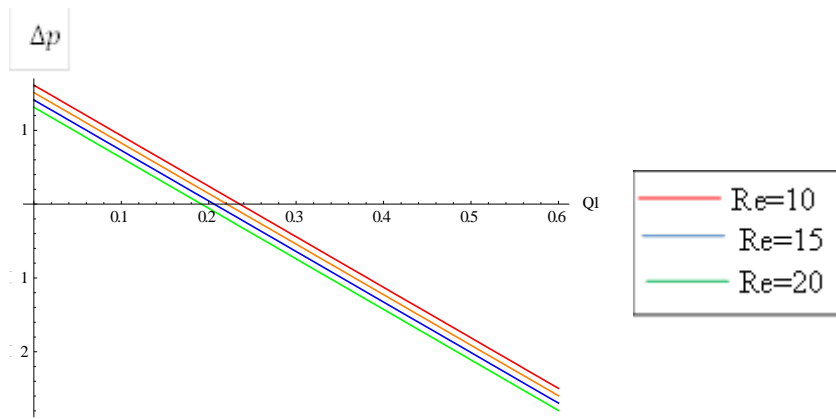


Figure 2- Pressure versus averaged flow rate for difference value of Re at Fr=0.1, $\lambda_1=1$, k= 0.1

$$\alpha^* = 0.2, \gamma = \frac{1}{2}, \phi = 0.5, \beta = 0.1.$$

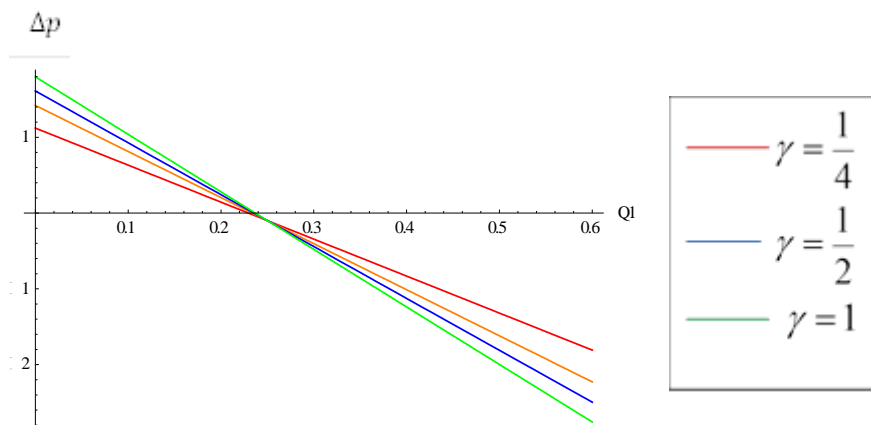


Figure 3- Pressure versus averaged flow rate for difference value of γ at Fr=0.1, Re=1, $\gamma = \frac{1}{4}=1$, k= 0.1 ,

$$\alpha^* = 0.2, \phi = 0.5, \beta = 0.1.$$

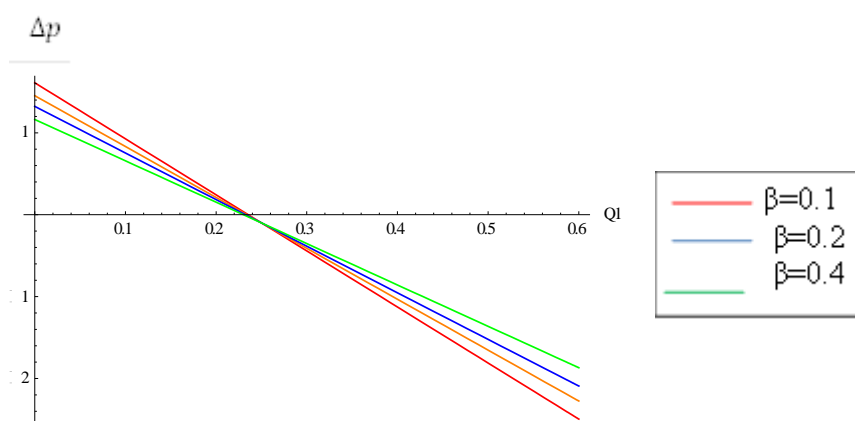


Figure 4- Pressure versus averaged flow rate for difference value of β at Fr=0.1, $\gamma = \frac{1}{4}=1$, Re= 1 , $\alpha^* = 0.2$,

$$\gamma = \frac{1}{2}, \phi = 0.5, k = 0.1.$$

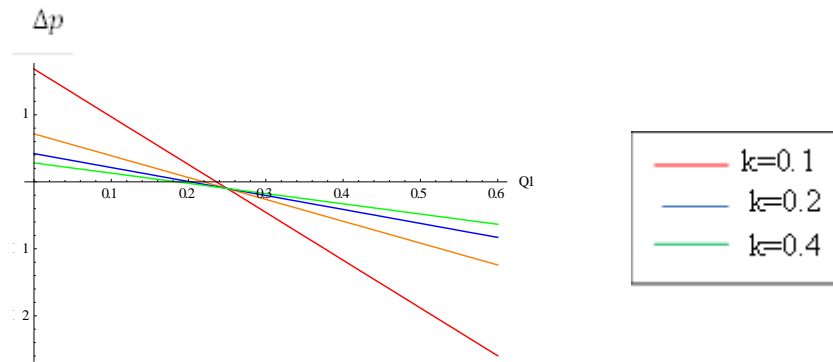


Figure 5- Pressure versus averaged flow rate for difference value of k at $Fr = 0.1, \gamma = \frac{1}{4} = 1, Re = 1, \alpha^* = 0.2, \gamma = \frac{1}{2}, \phi = 0.5, \beta = 0.1.$

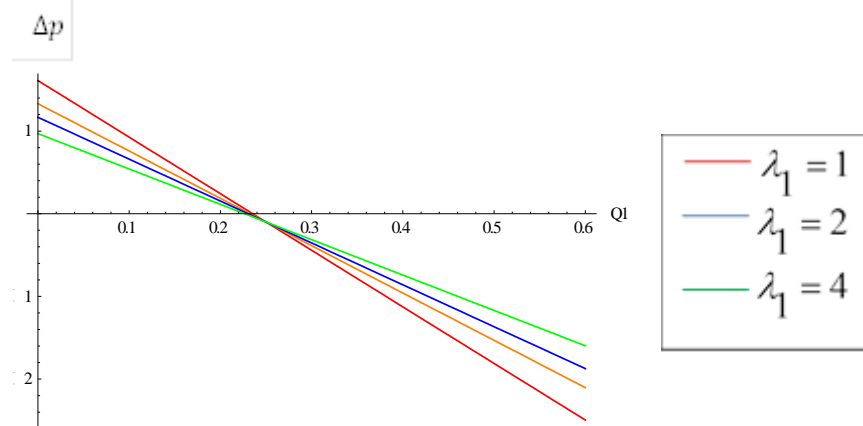


Figure 6- Pressure versus averaged flow rate for difference value of $\gamma = \frac{1}{4}$ at $Fr = 0.1, Re = 1, k = 0.1, \alpha^* = 0.2, \gamma = \frac{1}{2}, \phi = 0.5, \beta = 0.1.$

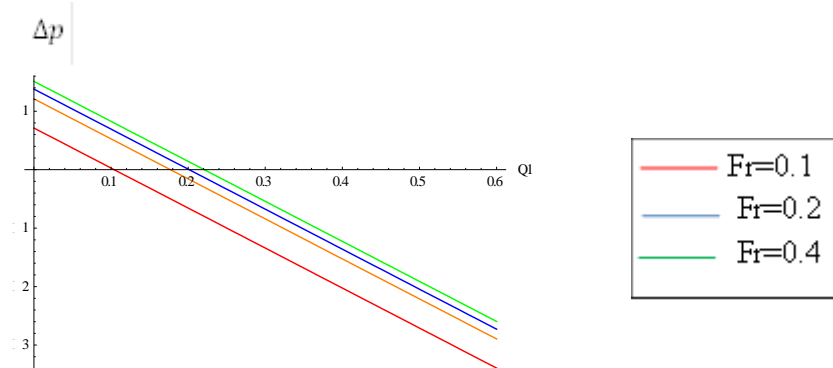


Figure 7- Pressure versus averaged flow rate for difference value of Fr at $Re = 1, \gamma = \frac{1}{4} = 1, k = 0.1, \alpha^* = 0.2, \gamma = \frac{1}{2}, \phi = 0.5, \beta = 0.1.$

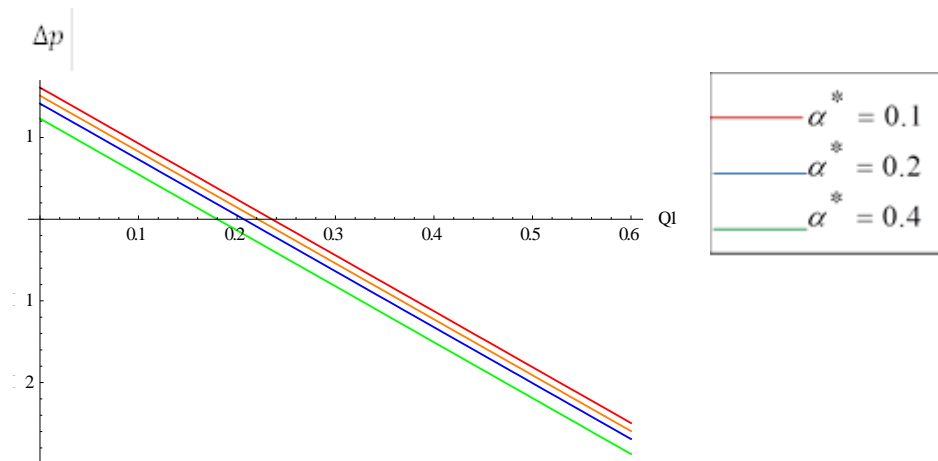


Figure 8- Pressure versus averaged flow rate for difference value of α^* at $Fr = 0.1, \gamma = \frac{1}{4} = 1, Re = 1, k = 0.1, \gamma = \frac{1}{2}, \phi = 0.5, \beta = 0.1$.

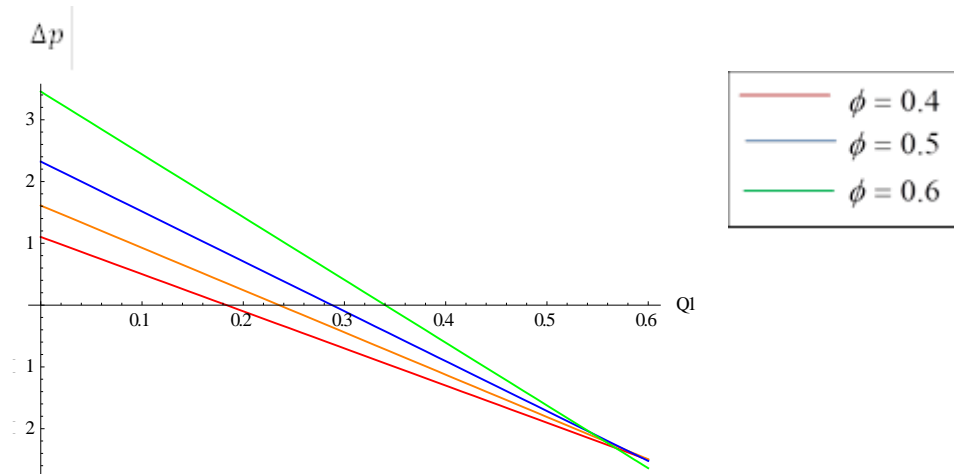


Figure 9- Pressure versus averaged flow rate for difference value of ϕ at $Fr = 0.1, \gamma = \frac{1}{4} = 1, k = 0.1, \alpha^* = 0.2, \gamma = \frac{1}{2}, Re = 1, \beta = 0.1$.

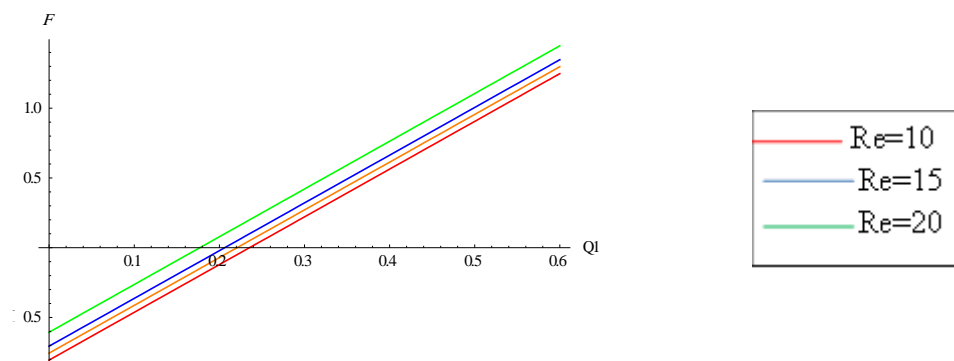


Figure 10- Fractional force versus averaged flow rate for difference value of Re at $Fr = 0.1, \gamma = \frac{1}{4} = 1, k = 0.1, \alpha^* = 0.2, \gamma = \frac{1}{2}, \phi = 0.5, \beta = 0.1$.

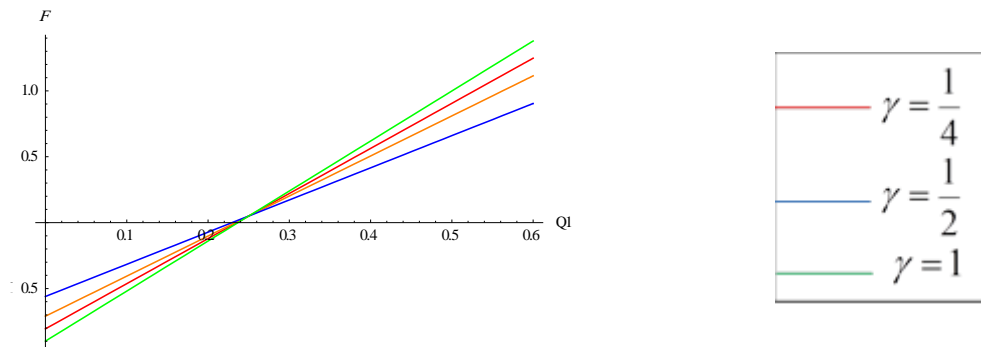


Figure 11- Fractional force versus averaged flow rate for difference value of γ at $Fr=0.1, Re=1, \gamma=\frac{1}{4}=1, k= 0.1, \alpha^*= 0.2 \ \phi =0.5, \beta=0.1$.

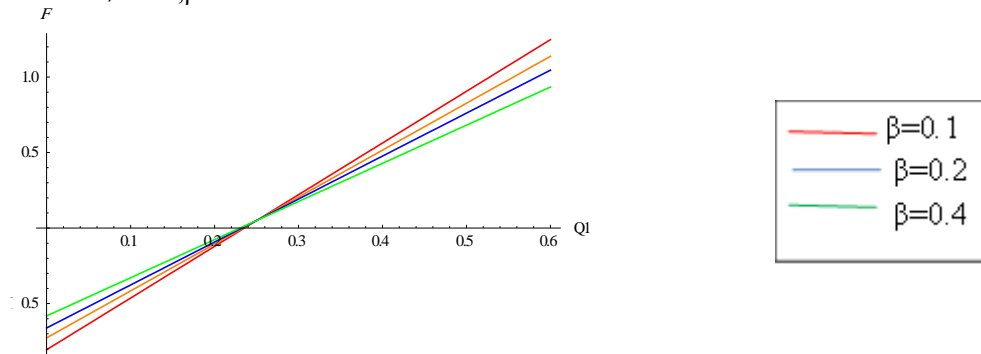


Figure 12- Fractional force versus averaged flow rate for difference value of β at $Fr =0.1, \gamma=\frac{1}{4}=1, Re= 1 ,$

$\alpha^* = 0.2 , \gamma = \frac{1}{2} , \phi =0.5, k=0.1.$

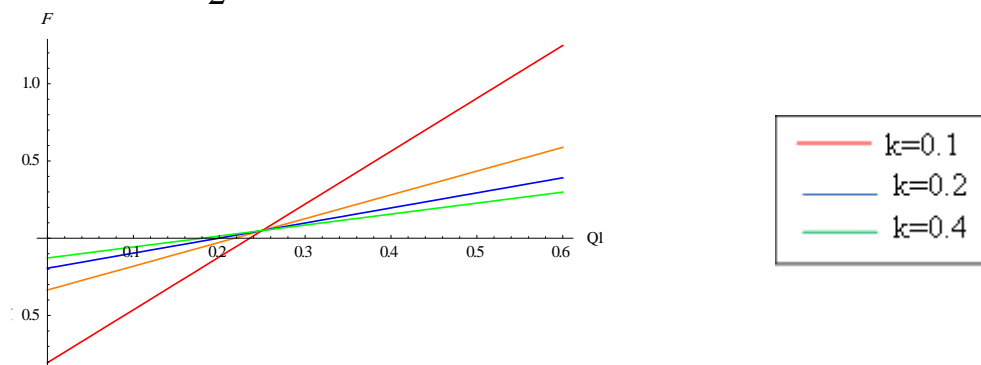


Figure 13- Fractional force versus averaged flow rate for difference value of k at $Fr =0.1, \gamma=\frac{1}{4}=1, Re= 1 ,$

$\alpha^* = 0.2 , \gamma=\frac{1}{2} , \phi =0.5, \beta=0.1.$

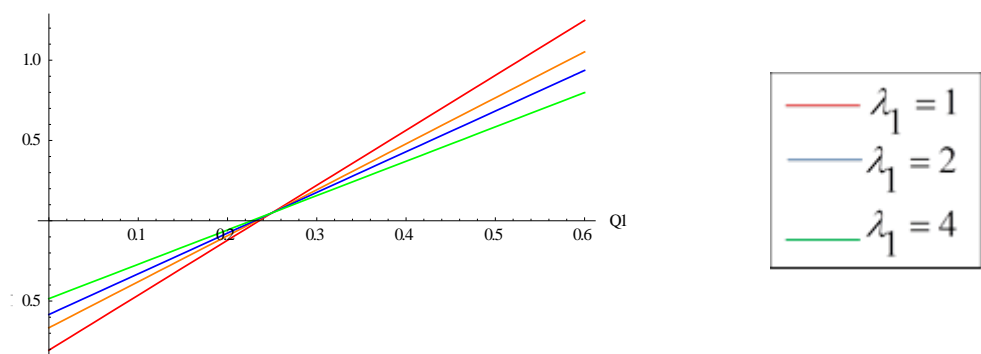


Figure 14- Fractional force versus averaged flow rate for difference value of $\gamma=\frac{1}{4}$ at $Fr=0.1, Re=1, k= 0.1, \alpha^*= 0.2, \gamma=\frac{1}{2} \ \phi =0.5, \beta=0.1.$

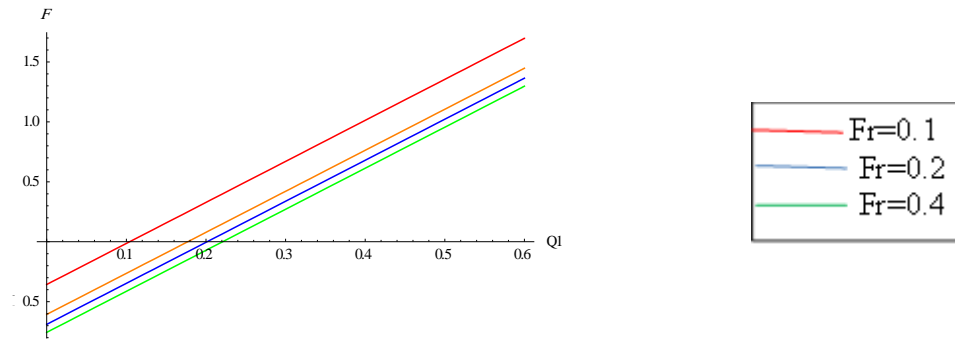


Figure 15- Fractional force versus averaged flow rate for difference value of Fr at $Re = 1, \gamma = \frac{1}{4} = 1, k = 0.1, \alpha^* = 0.2, \gamma = \frac{1}{2}, \phi = 0.5, \beta = 0.1$.

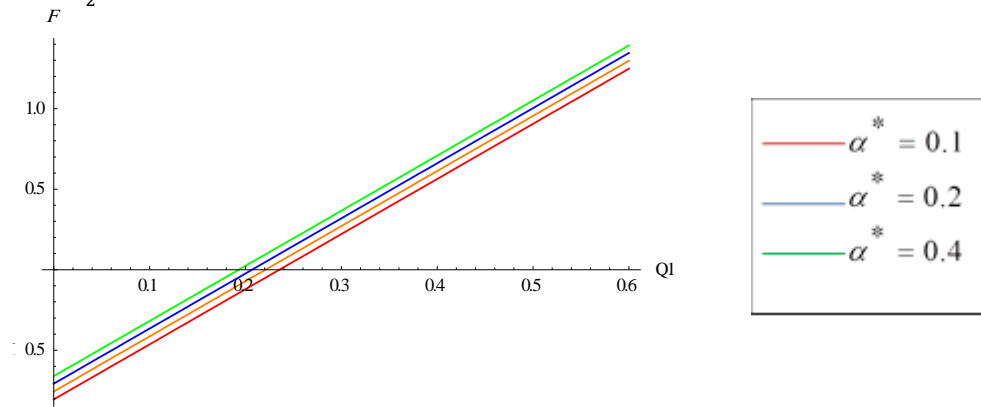


Figure 16- Fractional force versus averaged flow rate for difference value of α^* at $Fr = 0.1, \gamma = \frac{1}{4} = 1, Re = 1, k = 0.1, \gamma = \frac{1}{2}, \phi = 0.5, \beta = 0.1$.

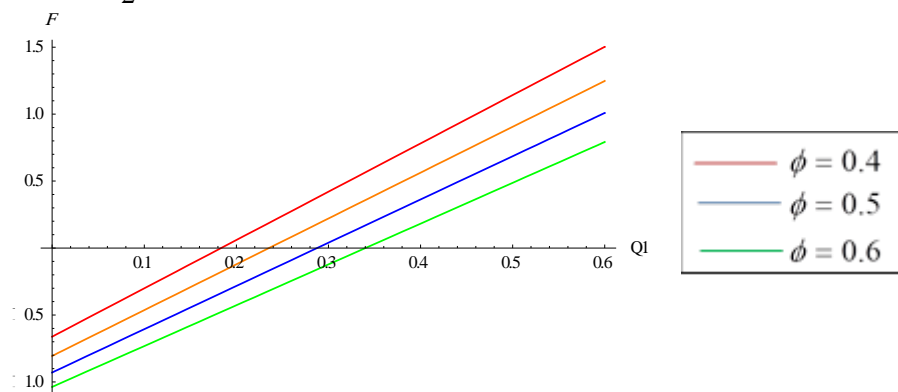


Figure 17- Fractional force versus averaged flow rate for difference value of ϕ at $Fr = 0.1, \gamma = \frac{1}{4} = 1, k = 0.1, \alpha^* = 0.2, \gamma = \frac{1}{2}, Re = 1, \beta = 0.1$.

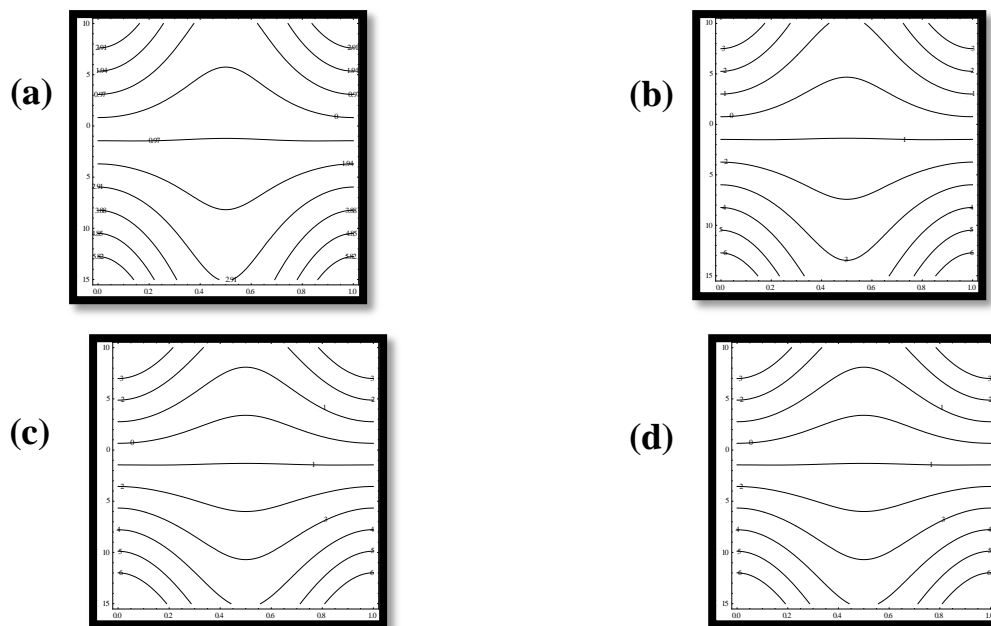


Figure 18- Streamline in the wave frame(axial coordinate. transverse coordinate for different value of Ha in $Q1 = . 5$ & $\phi = 0.5$ at (a) $k = 0.1$, (b) $k=0.2$, (c) $k=0.6$, (d) $k=0.8$ and the other parameter is $\beta=0.1$,

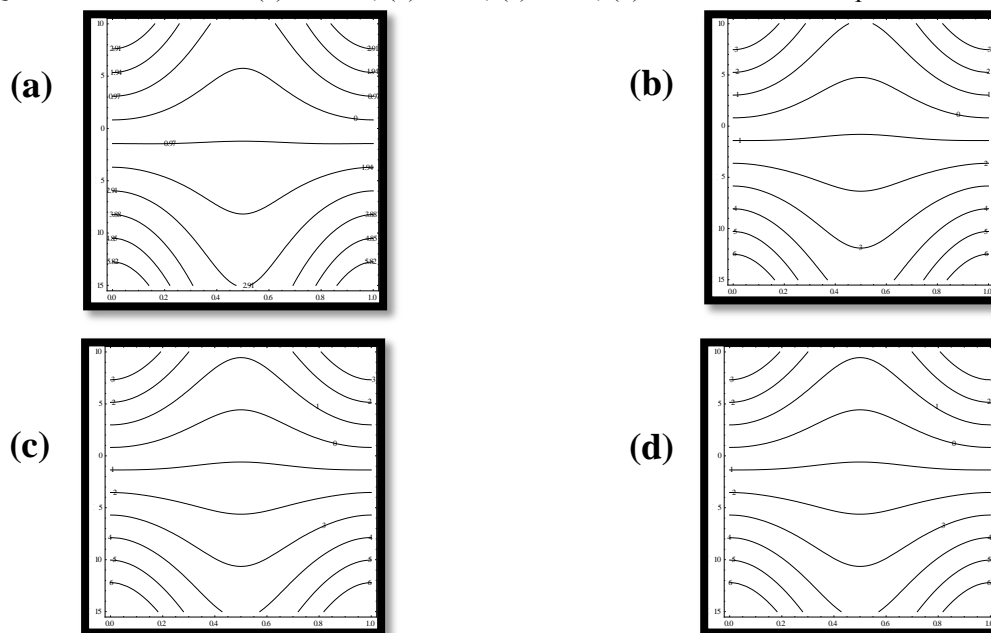


Figure 19- Streamline in the wave frame(axial coordinate. transverse coordinate for different value of Ha in $Q1 = . 5$ & $\phi = 0.5$ at (a) $\beta = 0.1$, (b) $\beta =0.2$, (c) $\beta =0.4$, (d) $Ha=0.6$ and the other parameter is $k = 0.1$,

Reference

1. Mainardi, F., Spada, G., and Creep. **2011**. Relaxation and viscosity properties for basic fractional models in rheology.*Eur. Physi.J.Special Top.*193, 133-160.
2. Liu, Y., Zheng, L., and Zhang, X. **2011**. Unsteady MHD Couette flow of a generalized Oldroyd-B fluid which fractional derivative. *Comput.Math.Appl.*61:443-450.
3. Nadeem, S. **2007**. General periodic flows of fractional Oldroyd-B fluid for anedge. *Phys.Lett.* A368:181-187.
4. Qi, H., and Jin, H. **2006**. Unsteady rotating flows of a viscoelastic fluid with the fractional Maxwell model between coaxial cylinders. *Acta Mech. Sin.*22:301-405.

5. Qi, H., and Xu. M. **2009**. Some unsteady unidirectional flows of a generalized Oldroyd-B fluid with fractional derivative. *Appl. Math. Model.* 33:4148-4191.
6. Tan, T., and Masuoka, W.C. **2007**. Stability analysis of a Maxwell fluid in a porous medium heated from below. *Phys. Lett. A* 360:454-460.
7. Vieru, D., and Fetecau, C. **2008**. Flow of a viscoelastic fluid with the fractional Maxwell model between two side walls perpendicular to a plate. *Appl. Math. Comput.* 200: 459-464.
8. Wang, Z. S., and Xu, M. **2009**. Axial Couette flow of two kinds of fractional viscoelastic fluids in an annulus. *Nonlinear Anal. Real World Appl.* 10:1087-1096.
9. Tripathi D. **2011**. Peristaltic flow of a fractional second grade fluid through a cylindrical tube, *Therm. Sci.*, 15:167-173.
10. Tripathi, D., Pandey, S.K., and Das, S. **2010**. Peristaltic flow of viscoelastic fluid with fractional Maxwell model through a channel. *Appl. Math. Comput.* 215:3645-3645.
11. Tripathi, D., Pandey, S.K., and Das, S. **2011**. Peristaltic transport of generalized Burgers' fluid. Application to the movement of chyme in small intestine. *Acta.Astron.* 69:30-38.
12. Bellman, R. **1964**. Perturbation Techniques in Mathematic, Physics and Engineering. *Holt. Rinehart and Winston*, New York.
13. Cole, J.D. **1968** .*Perturbation methods in Applied Mathematics*, Blaisedell, Waltham" AM.
14. Liu, G.L. **1997**. New research directions in singular perturbation theory. Artificial parameter approach and inverse-perturbation technique. Conference of 7th modern Mathematics and Mechanics, Shanghai.
15. He, J.H. **1998**. Approximate analytical solution for seepage flow with fractional derivatives in porous media. *J. Comput. Math. Appl. Mech. Eng.*, 167:57-68.
16. Joneidi AA, Domairry G., and Babaelahi, M. **2010**. Homotopy analysis method to Walter's B fluid in vertical channel with porous wall" *Meccanica.* 45(6): 857-868.
17. Ganji, D.D. **2006**. The application of He's homotopy perturbation method to nonlinear equations arising in heat transfer. *Phys. Lett. A*, 355:337-341.
18. Xue, C., and Nie, J. **2008**. Exact solutions of Rayleigh –Stokes problem for heated generalized Maxwell fluid in a porous half- space". *Math. Prob. Eng.* Article ID641431.
19. Tan, T., and Masuoka, W.C. **2007**. Stability analysis of a Maxwell fluid in a porous medium heated from below. *Phys. Lett. A* 360:454-460.